Separation of ethyl acetate and ethanol azeotropic system by acetate-based ionic liquid

Wenxiu Li
Shenyang University of Chemical Technology
Linzi Zhang
Shenyang University of Chemical Technology
Xin He
Shenyang University of Chemical Technology
Qingfeng Ni
Shenyang University of Chemical Technology
Tao Zhang
taozhang151@126.com

Shenyang University of Chemical Technology

Research Article

Keywords: vapor-liquid equilibrium, ethyl acetate, NRTL model, ethanol, ionic liquids

Posted Date: June 29th, 2023

DOI: https://doi.org/10.21203/rs.3.rs-3109611/v1

Additional Declarations: No competing interests reported.

Version of Record: A version of this preprint was published at Journal of Solution Chemistry on March 28th, 2024. See the published version at https://doi.org/10.1007/s10953-023-01361-5.

Separation of ethyl acetate and ethanol azeotropic system by acetate-based ionic liquid

Wenxiu Li, Linzi Zhang, Xin He, Qingfeng Ni, Tao Zhang*

Liaoning Provincial Key Laboratory of Chemical Separation Technology, Shenyang University of Chemical Technology, Shenyang, 110142, China.

*corresponding author. Tel.: +8602489381082. E-mail address: taozhang151@126.com

Abstract

Three ionic liquids （ILs）(1-ethyl-2,3-dimethylimidazolium acetate, [EMMIM][AC]; tributyl-methylammonium acetate, $[N_{4,4,4,1}][AC]$; and tetraethylammonium acetate, $[N_{2,2,2,2}][AC]$) were chosen. The vapor-liquid equilibrium (VLE) data of ternary mixtures (acetate + ethanol + IL) were gauged at 101.3KPa. NRTL equation was applied to correlate the data. From NRTL model, for $[N_{2,2,2,2}][AC]$, [EMMIM][AC] and $[N_{4,4,4,1}][AC]$, minimum mole fractions for completely eliminating azeotrope are 0.015, 0.020 and 0.022, respectively. From the average relative volatility and σ-profiles, it can be obtained that the separation ability order is [EMMIM][AC] > $[N_{2,2,2,2}][AC]$ > $[N_{4,4,4,1}][AC]$.

Keywords vapor-liquid equilibrium; ethyl acetate; NRTL model; ethanol; ionic liquids

List of symbols

x_i	Liquid phase mole fraction of constituent i
y_i	Vapor phase mole fraction of constituent i
x'_i	Liquid phase mole fraction of constituent i excluding IL
P	Total pressure in the equilibrium system
P_i^0	Saturated vapor pressure of constituent i
t	Equilibrium temperature in ℃
A_i, B_i, C_i	Antoine parameters of constituent i
x_3	Liquid phase mole fraction of IL
n	Amount of experimental data points
exp	Experimental values
calc	Calculated values
K	K-th data point

Greek letters

α_{12}	Relative volatility of constituent 1 to constituent 2
α_{ij}	Nonstochastic parameters of NRTL model
γ_i	The activity coefficient of constituent *i*

1 Introduction

In chemical production, ethyl acetate and ethanol are basic chemical products that are in high demand [1,2]. At atmospheric pressure, ethyl acetate and ethanol exist as azeotrope, and this azeotrope is widely present in the crude product of ethyl acetate [3,4]. To find an efficient separation method, many previous studies were reported [5-7]. Extractive distillation has received extensive attention due to its simple operation and wide adjustable range. The cost of the unit operation can be greatly reduced by choosing a good extractant, so the extractant is the focus of the extractive distillation operation unit [8-15]. IL can be used as an extractant in the operation which have the same good extraction effect as traditional extractants (organic solvents and solid salts), but without the disadvantages of volatile, physical and chemical instability and corrosion of pipelines [16-21]. Up to now, with the development of industry, the separation of azeotrope using ILs as extractants has been widely covered in a large number of prints [22-37].

Many ILs (e.g., [BMIM][DBP], [EMIM][$MeSO_3$], [EMIM][BF_4], [OMIM][BF_4], [EMIM][AC], [EMIM][$FCSO_3$], [BMIM][$FCSO_3$], [EMIM][$MeSO_4$], [EMIM][Tf_2N], [HMIM][Tf_2N], [MMIM][DMP], [OMIM][PF6]) have been utilized to separate the binary azeotrope [4,21-26]. The minimum molar fractions of azeotropic destruction by the ILs are from 0.025 to 0.3 [25].

The high accuracy has been shown in screening ILs for azeotrope separation by COSMO-RS method [38-49]. COSMOthermX software has been used by J. Dhanalakshmi etc for selecting IL to separate the mixture studied in this manuscript. According to the relative volatility calculated through the COSMOthermX software, the separation effect of [DHP]-, [Cl]- and [OAc]- on the system is obviously better than that of other anions. Compared with pyridine, pyrrolidine and quinoline cations, imidazolyl cations have greater separation effects [31].

In this manuscript, ILs were selected primarily by their solubility and selectivity in the constituents to be separated using the COSMOthermX software. Detailed procedures are presented in the Supporting Information [50-53]. Three ILs ([$N_{2,2,2,2}$][AC]; [EMMIM][AC] and [$N_{4,4,4,1}$][AC]) were obtained as extractants for the experiments. The measured VLE data were fitted by the NRTL equation. The minimum breaking azeotropic concentration and the average relative volatility were used to evaluate the IL separation ability. σ-profile was used to analyze the separation mechanism.

2 Experimental

2.1 Chemical supplies

High purity ethyl acetate and ethanol (99.5%, wt) were gained from Sinopharm Group. ILs (99.0%, wt) were bought from YuLu Group, which meets the purity requirement of the experiment. Volatile impurities in ILs need to be cleaned, they were dried for 36 h at 333 k and 2 kPa. The exact amount of water in the ILs can be obtained by the method of Karl Fischer, where the mass fraction of water is less than 0.005. Specific information about these chemicals is shown in Table 1.

Table 1 The Chemical Samples specifications

Chemical name	CAS	supplier	mass fraction	Water content (ppm)	Purification method	Analysis method[a]
ethanol	64-17-5	Sinopharm Group	0.995	none	None	GC
ethyl acetate	141-78-6	Sinopharm Group	0.995	none	None	GC
[$N_{2,2,2,2}$][AC][b]	1185-59-7	Yulu Group	0.990	<500	Vacuum	KF LC

[EMMIM][AC][c]	141085-38-3	Yulu Group	0.990	<500	desiccation Vacuum desiccation	KF LC
$[N_{4,4,4,1}][AC]$[d]	131242-39-2	Yulu Group	0.990	<500	Vacuum desiccation	KF LC

[a]GC = gas chromatography; LC = liquid chromatograph; KF = Karl Fischer titration. [b]$[N_{2,2,2,2}][AC]$ = tetraethylammonium acetate. [c][EMMIM][AC] = 1-ethyl-2,3-dimethylimidazolium acetate. [d]$[N_{4,4,4,1}][AC]$ = tributyl-methylammonium acetate.

2.2 Procedure and Apparatus

Complete the VLE experiment by using a circulation VLE kettle (NGW, Wertheim, Germany) and obtain the phase equilibrium experimental data. The experimental setup diagram had been introduced in previous article. [27] The given liquid sample is heated in the boiling chamber. A press gauge is used. The vacuum pump (SHZ-DIII FANGYUAN China), buffer and N_2 vessel are connected to the experimental setup to stabilize the pressure at 101.3 kPa [28]. The thermograph is calibrated by the Shenyang measurement and testing center using the external standard method. In this experiment, each sample used in the VLE experiment is prepared by gravimetric analysis in virtue of an electronic scale (CAV264C OHAUS America). The standard uncertainties of press gauge, thermograph and electronic scale are 0.1kPa, 0.5K and 0.0001g, respectively.

A headspace sampler (G1888, Agilent Technologies) connected with a GC (model 7890A, Agilent Technologies) is utilized to gauge the ethyl acetate and ethanol contents. GC is performed using Agilent 19091J-413 capillary column (30 m × 0.32 mm, 0.25 μm) and flame ionization detector (FID). The temperature of column, injector and detector are 343.15K, 493.15K, and 523.15K, respectively. The IL molar content is measured by differential gravimetric method, which is due to the low vapor pressure of IL [10]. The standard molar uncertainty of this constituent is 0.002. Each sample needs to be measured more than three times.

2.3 Data Processing

On account of the low pressure, the ideal steam hypothesis is proposed. Raoult's law of non-ideal solution can be written as formula (1). [54].

$$\gamma_i = \frac{Py_i}{P_i^0 x_i} \quad (1)$$

x_i, and y_i are molar fraction of constituent i in liquid phase and vapor phase, respectively. The activity coefficient of constituent i is written as γi. The total pressure is written as P. The Eq. 2 [6,55] can be utilized to estimate saturated vapor pressure at t ℃. Antoine Parameters (Ai, Bi and Ci) are gained from reference [6].

$$\ln P_i^0 = A_i - \frac{B_i}{t+C_i} \quad (2)$$

Table 2 Antoine Parameters of pure constituent

constituent	A	B	C
ethanol[b]	16.83	3758.56	-43.78
ethyl acetate[b]	14.22	2799.54	-58.92

[a]Antoine equation ln(p/kpa) = A-B/(t/K+C), [b]Parameters gained from Ref.[6]

Eq. 3 can be used to calculate relative volatility (α_{12}). [56]

$$\alpha_{12} = \frac{y_1/x_1}{y_2/x_2} = \frac{p_1^0 \gamma_1}{p_2^0 \gamma_2} \quad (3)$$

Where 1 represents ethyl acetate and 2 represents ethanol. Average relative volatility ($\overline{\alpha_{12}}$) is shown down here. [57]

$$\overline{\alpha_{12}} = \int_{x_1'=0}^{x_1'=1} \alpha_{12}\, dx_1' \tag{4}$$

Liquid phase mole fraction of ethyl acetate excluding IL is expressed by x_1'.

$$x_1' = \frac{x_1}{(1-x_3)} \tag{5}$$

The six energy parameters, $\triangle g_{12}$ and $\triangle g_{21}$ in a group, in the same way $\triangle g_{23}$ and $\triangle g_{32}$, $\triangle g_{13}$ and $\triangle g_{31}$, and the three non-random action parameters α_{12}, α_{13}, α_{23} in the NRTL thermodynamic are obtained using Eq.6 [59,60] to minimize the objective function (ARD). This method was developed from the Levenberg-Marquardt method [45]

$$ARD(\%) = \frac{1}{n}\sum_1^n \sum_1^2 \left|\frac{\gamma_i^{exp} - \gamma_i^{calc}}{\gamma_i^{exp}}\right| \times 100 \tag{6}$$

The thermodynamics consistency of the binary system VLE data is verified by Fredenslund's test and Wisniak's L-W test [61-63].

The separation mechanism is derived from σ- profiles [31]. The σ profile consists of three parts, which bounded by $|\sigma| = 0.0082 e/Å^2$ are the donor region, the non-polar region and the receptor region in turn， from left to right [29]. The strength of hydrogen bonds is mainly related to the area size of the ion peak.

3 Result and Discussion

3.1 Measurement of the Experimental Setup reliability

At 101.3kpa, the ethanol-ethyl acetate VLE data were gauged in this experiment and listed in Table 3. The purpose is to estimate the laboratory device reliability. The experimental data and the data reported are displayed in Figure 1(a)-1(b) [3,4].

In Figure 1(a)-1(b), the values obtained in this experiment are basically consistent with those recorded in the reference 3. The deviations of the two literatures data are large. The thermodynamic consistency test is also used to estimate reliability of the measurement results. The value distribution of $y_i^{exp} - y_i^{calc}$ can be seen from Figure 2. The calculated result of Fredenslund's test is $\sum_{i=1}^{n} \frac{\left|y_i^{exp} - y_i^{calc}\right|}{n-2} = 0.0003 < 0.008$ and that of the Wisniak L-W test is F=3.9<5. The thermodynamic consistency is reached by using the binary data. So the reliability of experiment method and instrument is proved [28,29].

Table 3 Isobaric VLE Data for Binary System of Ethyl Acetate (1) + Ethanol (2) at 101.3 kPa[a]

T/K	x_1'	y_1	α_{12}	γ_1	γ_2
350.89	0.019	0.039	2.095	2.026	1.006
350.53	0.033	0.067	2.104	2.028	1.005
349.77	0.069	0.128	1.981	1.899	1.006
349.02	0.108	0.185	1.875	1.798	1.012
348.21	0.155	0.25	1.817	1.739	1.015
347.47	0.206	0.298	1.636	1.599	1.042
346.79	0.264	0.35	1.501	1.499	1.071
346.25	0.323	0.401	1.403	1.430	1.097
345.75	0.393	0.448	1.254	1.336	1.151
345.31	0.492	0.512	1.083	1.238	1.238
345.25	0.575	0.564	0.956	1.169	1.325

345.52	0.658	0.621	0.852	1.115	1.415
346.21	0.746	0.684	0.737	1.058	1.544
346.89	0.815	0.746	0.667	1.032	1.658
347.73	0.882	0.818	0.601	1.017	1.799
348.73	0.932	0.886	0.567	1.008	1.878

[a]Standard uncertainty u are u (x_1) = u (y_1) = 0.002, u (T) = 0.5 K, u (P) = 0.1 kPa.

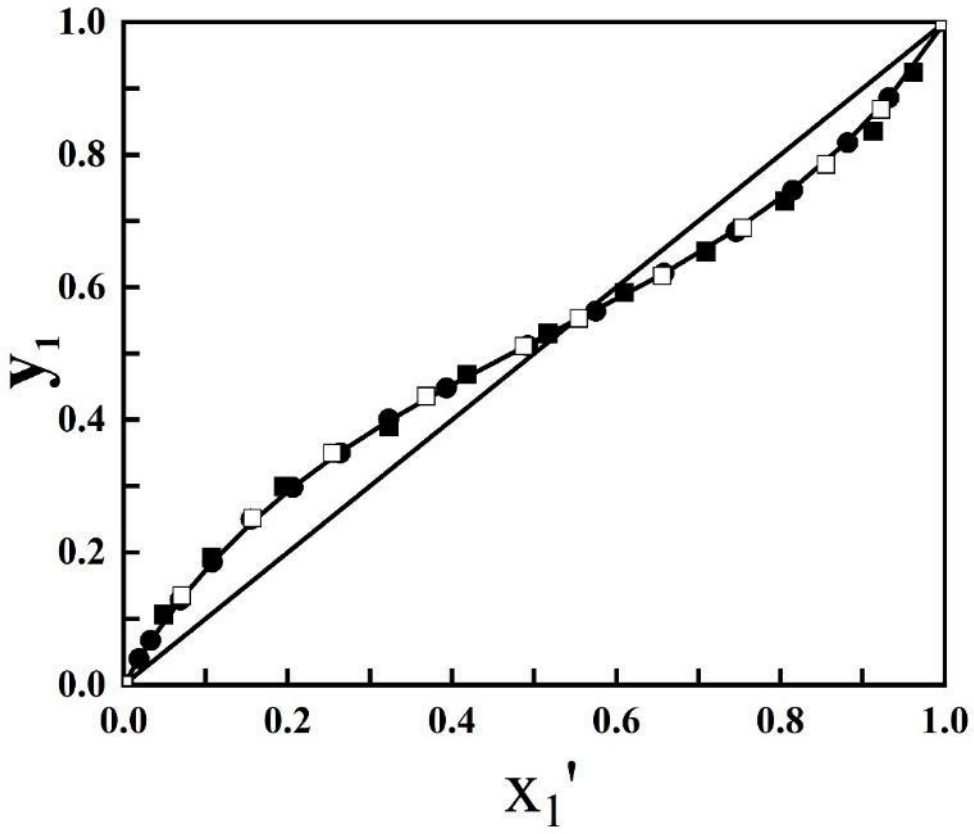

Fig. 1(a) x_1'-y_1 diagram for the binary system of ethyl acetate (1) + ethanol (2) at 101.3 kPa: ●, experimental data; □, from ref 3; ■, from ref 4; solid line, correlated using the NRTL model.

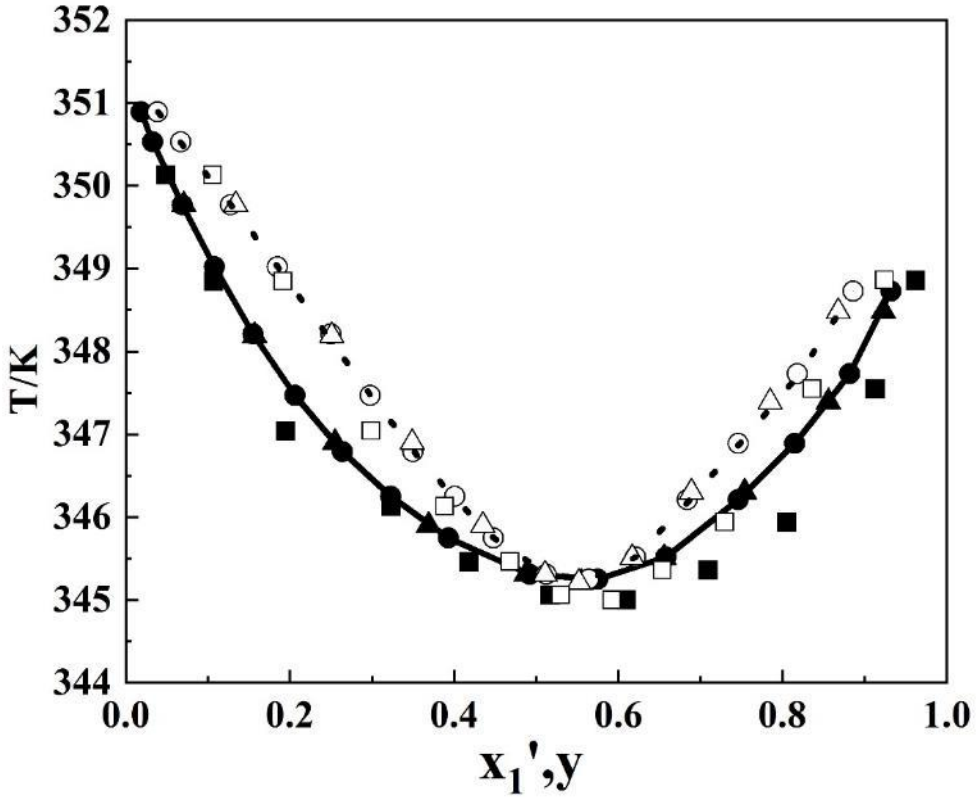

Fig. 1(b) The T-x_1'-y_1 diagram for binary system ethyl acetate (1) + ethanol (2) at 101.3 kPa: (●, O)T-x_1', T-y_1 experimental data; (▲, Δ) T-x_1', T-y_1 data from ref 3; (■, □) T-x_1', T-y_1 data from ref 4; solid line, T-x_1' data correlated using NRTL model; dashed line, T-y_1 data correlated using NRTL model.

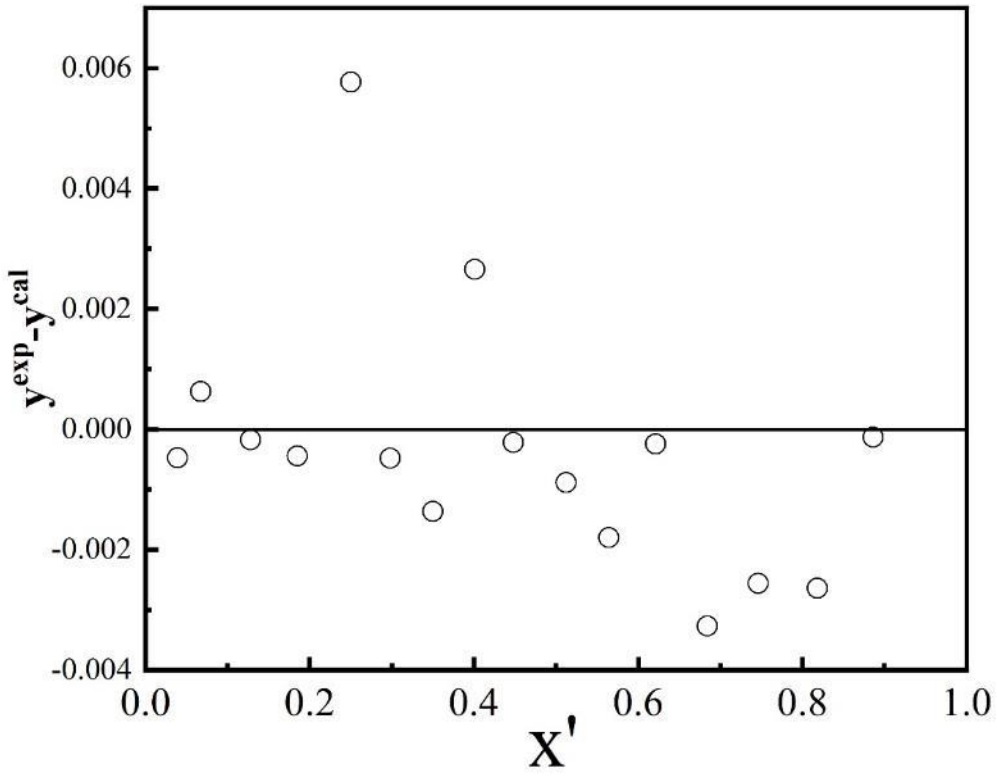

Fig. 2 Vapor composition residuals diagram for the binary system of ethyl acetate (1) + ethanol (2) at 101.3 kPa.

3.2. Experiment Data

The ethyl acetate + ethanol + $[N_{2,2,2,2}][AC]$ (a), [EMMIM][AC] (b) or $[N_{4,4,4,1}][AC]$ (c) VLE data at one atmosphere are displayed in Tables 4-6 and Figures 3-7. The IL molar fractions of the ternary mixtures are 0.06, 0.03 and 0.01. The interaction parameters and ARD are indicated in Table 7. From table 7 and figures 3-7, the conclusion can be inferred that NRTL equation has a good correlation with experiment results. [64,65].

Table 4 VLE Data of the Ternary Ethyl Acetate (1) + Ethanol (2) + $[N_{2,2,2,2}][AC]$ (3) System at 101.3 kPa[a]

x_3	T/K	x_1	x_1'	y_1	α_{12}	γ_1	γ_2
0.009	349.61	0.967	0.976	0.97	0.795	1.032	1.364
0.009	348.41	0.903	0.911	0.892	0.807	1.059	1.390
0.009	347.31	0.806	0.813	0.788	0.855	1.087	1.358
0.010	346.52	0.690	0.697	0.69	0.968	1.142	1.267
0.010	346.17	0.574	0.580	0.606	1.114	1.219	1.178
0.009	346.05	0.475	0.479	0.532	1.236	1.300	1.133
0.010	346.25	0.386	0.390	0.469	1.381	1.400	1.090
0.011	346.89	0.292	0.295	0.398	1.580	1.538	1.042
0.009	347.61	0.234	0.236	0.343	1.690	1.614	1.017
0.010	348.30	0.184	0.186	0.293	1.814	1.711	1.000
0.011	348.95	0.145	0.147	0.247	1.903	1.788	0.991
0.010	349.85	0.099	0.100	0.183	2.016	1.888	0.982
0.011	350.69	0.054	0.055	0.11	2.124	2.009	0.986
0.030	349.77	0.863	0.890	0.916	1.348	1.087	0.846
0.031	349.00	0.812	0.838	0.871	1.305	1.127	0.911

0.032	348.31	0.751	0.776	0.821	1.324	1.175	0.941
0.032	347.62	0.665	0.687	0.749	1.360	1.239	0.971
0.031	347.19	0.564	0.582	0.667	1.439	1.320	0.980
0.030	347.06	0.467	0.481	0.589	1.546	1.415	0.979
0.032	347.23	0.359	0.371	0.511	1.772	1.586	0.956
0.031	347.69	0.283	0.292	0.441	1.913	1.711	0.952
0.030	348.29	0.222	0.229	0.375	2.020	1.816	0.953
0.030	349.11	0.157	0.162	0.296	2.175	1.972	0.955
0.032	349.81	0.115	0.119	0.238	2.312	2.113	0.958
0.030	350.39	0.085	0.088	0.188	2.399	2.210	0.962
0.031	351.29	0.046	0.047	0.111	2.532	2.374	0.973
0.060	349.44	0.761	0.810	0.911	2.401	1.239	0.542
0.060	348.96	0.712	0.757	0.875	2.247	1.294	0.607
0.061	348.60	0.653	0.695	0.831	2.158	1.356	0.665
0.061	348.23	0.582	0.619	0.776	2.132	1.439	0.716
0.060	348.07	0.493	0.524	0.703	2.150	1.547	0.764
0.061	348.10	0.400	0.426	0.628	2.275	1.700	0.793
0.062	348.27	0.337	0.358	0.573	2.406	1.837	0.809
0.061	348.77	0.257	0.273	0.487	2.528	2.011	0.840
0.060	349.41	0.200	0.213	0.417	2.643	2.158	0.859
0.061	350.33	0.150	0.160	0.345	2.765	2.308	0.872
0.060	351.07	0.112	0.119	0.276	2.822	2.421	0.892
0.059	351.67	0.090	0.096	0.233	2.861	2.481	0.898
0.060	352.49	0.069	0.073	0.187	2.921	2.553	0.900

Table 5 VLE Data of the Ternary Ethyl Acetate (1) + Ethanol (2) + [EMMIM][AC] (3) System at 101.3 kPa[a]

x_3	T/K	x_1	x_1'	y_1	α_{12}	γ_1	γ_2
0.01	349.17	0.915	0.924	0.900	0.740	1.028	1.463
0.01	348.22	0.848	0.857	0.826	0.792	1.050	1.406
0.009	347.43	0.780	0.787	0.758	0.848	1.076	1.354
0.011	346.73	0.683	0.691	0.688	0.986	1.141	1.241
0.012	346.32	0.593	0.600	0.625	1.111	1.212	1.173
0.010	346.23	0.483	0.488	0.543	1.247	1.296	1.118
0.011	346.54	0.378	0.382	0.472	1.446	1.425	1.058
0.010	347.05	0.301	0.304	0.408	1.578	1.520	1.030
0.010	347.67	0.235	0.237	0.348	1.718	1.629	1.009
0.012	348.24	0.155	0.157	0.266	1.946	1.848	1.007
0.010	348.90	0.117	0.118	0.212	2.011	1.913	1.004
0.010	349.54	0.091	0.092	0.173	2.065	1.960	0.998
0.012	350.15	0.074	0.075	0.148	2.142	2.020	0.986
0.029	349.50	0.838	0.863	0.890	1.284	1.097	0.898
0.030	348.72	0.789	0.813	0.850	1.303	1.143	0.927
0.030	347.96	0.730	0.753	0.804	1.346	1.197	0.945
0.031	347.30	0.645	0.666	0.741	1.435	1.277	0.950
0.030	346.95	0.548	0.565	0.667	1.542	1.369	0.950
0.031	346.68	0.453	0.467	0.596	1.684	1.496	0.952
0.030	346.85	0.349	0.360	0.514	1.880	1.662	0.947
0.031	347.34	0.274	0.283	0.441	1.999	1.786	0.954
0.031	348.01	0.215	0.222	0.379	2.139	1.913	0.950
0.030	348.78	0.152	0.157	0.295	2.247	2.050	0.964
0.030	349.55	0.112	0.115	0.232	2.325	2.145	0.970
0.031	350.40	0.082	0.085	0.185	2.444	2.253	0.963
0.030	351.71	0.045	0.046	0.110	2.563	2.369	0.956
0.061	349.82	0.715	0.761	0.888	2.490	1.270	0.535
0.060	348.96	0.669	0.712	0.859	2.464	1.350	0.579
0.060	348.33	0.614	0.653	0.822	2.454	1.439	0.621

0.061	347.81	0.546	0.582	0.780	2.546	1.560	0.652
0.062	347.50	0.462	0.493	0.719	2.631	1.717	0.696
0.062	347.43	0.375	0.400	0.644	2.713	1.900	0.747
0.061	347.66	0.316	0.337	0.582	2.739	2.021	0.786
0.061	348.11	0.241	0.257	0.499	2.880	2.238	0.825
0.060	348.88	0.188	0.200	0.424	2.944	2.379	0.853
0.061	350.21	0.141	0.150	0.351	3.065	2.515	0.858
0.060	351.12	0.105	0.112	0.280	3.083	2.605	0.878
0.059	351.71	0.085	0.090	0.233	3.072	2.643	0.891
0.060	352.61	0.065	0.069	0.188	3.124	2.705	0.890

Table 6 VLE Data of the Ternary Ethyl Acetate (1) + Ethanol (2) + $[N_{4,4,4,1}][AC]$ (3) System at 101.3 kPa[a]

x_3	T/K	x_1	x_1'	y_1	α_{12}	γ_1	γ_2
0.009	349.30	0.925	0.933	0.906	0.692	1.019	1.550
0.010	348.36	0.857	0.866	0.832	0.766	1.041	1.440
0.010	347.67	0.787	0.795	0.765	0.839	1.068	1.354
0.011	346.94	0.690	0.698	0.687	0.950	1.120	1.263
0.012	346.49	0.600	0.607	0.626	1.084	1.193	1.182
0.011	346.15	0.488	0.493	0.543	1.222	1.288	1.134
0.010	346.23	0.382	0.386	0.466	1.388	1.406	1.090
0.011	346.73	0.305	0.308	0.407	1.542	1.515	1.053
0.010	347.33	0.238	0.240	0.345	1.668	1.613	1.032
0.011	348.56	0.157	0.159	0.260	1.858	1.763	1.004
0.010	349.12	0.119	0.120	0.209	1.938	1.841	1.001
0.011	349.68	0.092	0.093	0.171	2.011	1.910	0.996
0.010	350.05	0.075	0.076	0.144	2.045	1.942	0.994
0.03	350.57	0.837	0.863	0.879	1.153	1.047	0.947
0.029	349.68	0.790	0.814	0.836	1.165	1.086	0.979
0.029	348.97	0.731	0.753	0.787	1.212	1.132	0.985
0.030	348.37	0.671	0.692	0.743	1.287	1.188	0.978
0.030	347.55	0.587	0.605	0.679	1.381	1.276	0.985
0.030	347.15	0.470	0.485	0.591	1.534	1.404	0.978
0.031	347.05	0.380	0.392	0.521	1.687	1.538	0.975
0.031	347.38	0.319	0.329	0.468	1.794	1.628	0.968
0.030	347.96	0.203	0.209	0.347	2.011	1.862	0.984
0.029	348.84	0.137	0.141	0.260	2.141	2.006	0.989
0.029	349.66	0.101	0.104	0.205	2.222	2.086	0.986
0.030	350.81	0.055	0.057	0.124	2.342	2.219	0.987
0.030	351.69	0.028	0.029	0.067	2.404	2.290	0.986
0.061	350.51	0.803	0.855	0.932	2.324	1.160	0.521
0.060	349.31	0.723	0.769	0.880	2.203	1.266	0.605
0.060	348.61	0.659	0.701	0.837	2.190	1.352	0.653
0.061	348.03	0.572	0.609	0.776	2.224	1.472	0.703
0.059	347.83	0.491	0.522	0.705	2.188	1.568	0.762
0.059	347.97	0.409	0.435	0.633	2.240	1.681	0.797
0.060	348.21	0.353	0.375	0.583	2.330	1.784	0.812
0.061	348.73	0.268	0.285	0.494	2.449	1.957	0.844
0.060	349.57	0.193	0.205	0.394	2.521	2.108	0.878
0.061	350.43	0.144	0.153	0.321	2.617	2.239	0.893
0.062	351.29	0.107	0.114	0.257	2.688	2.341	0.904
0.060	352.08	0.080	0.085	0.199	2.674	2.364	0.913
0.061	353.14	0.051	0.054	0.135	2.734	2.442	0.915

[a]Standard uncertainty u (x_1) = u (y_1) = 0.002, u (T) = 0.5 K, u (P) = 0.1 kPa, y_3 = 0

Table 7 Non-random action parameters α_{ij}, energy parameters Δg_{ij} Δg_{ji} and ARD of the NRTL Model

Constituent i	Constituent j	α_{ij}	Δg_{ij}(J/mol)	Δg_{ji}(J/mol)	ARD(%)
ethyl acetate	ethanol	0.204	795.309	1412.033	1.448
ethyl acetate	$[N_{2,2,2,2}][AC]$	0.632	-8339.183	-2862.760	1.519
ethanol	$[N_{2,2,2,2}][AC]$	0.301	-30872.941	-9799.878	
ethyl acetate	[EMMIM][AC]	0.414	354.750	-7216.402	0.717
ethanol	[EMMIM][AC]	0.061	-31820.230	-20656.690	
ethyl acetate	$[N_{4,4,4,1}][AC]$	0.612	-12382.190	-5959.333	1.014
ethanol	$[N_{4,4,4,1}][AC]$	0.200	-47087.719	-10638.902	

Figure 3 is the $x_1' - y_1$ diagram of the ternary data from tables 4-6. The azeotropic point enhances with enhance of IL content in mixed solution, and no azeotropic point is present at IL molar fraction of 0.03. From the NRTL model, for $[N_{2,2,2,2}][AC]$, [EMMIM][AC] and $[N_{4,4,4,1}][AC]$, minimum mole fractions for completely eliminating azeotrope are 0.015, 0.020 and 0.022, respectively. Compared to previously reported results, the range of that is from 0.025 to 0.3[4,21-26], the better breaking azeotropic capacities are shown by the three ILs. According to Tables 4-6 and Figure 4, the VLE temperature is changed synchronously with IL mole fraction.

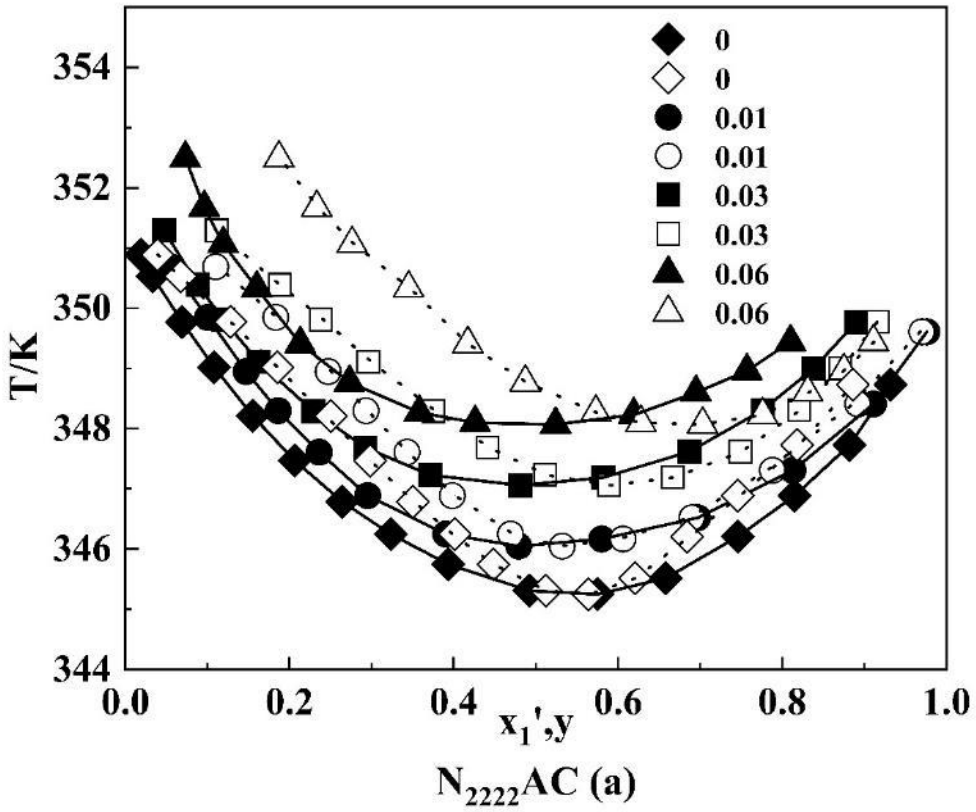

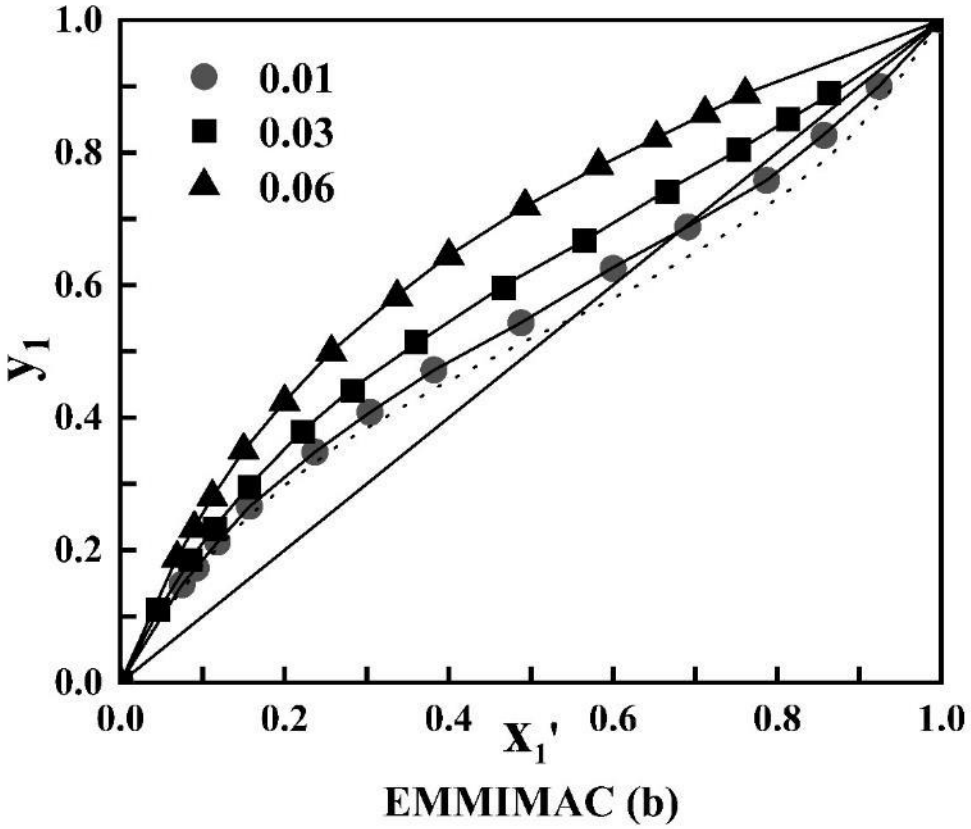
1.0
0.8
0.6
0.4
0.2
0.0
0.0
0.2
0.4
0.6
0.8
1.0
y1
x1'
0.01
0.03
0.06
EMMIMAC (b)

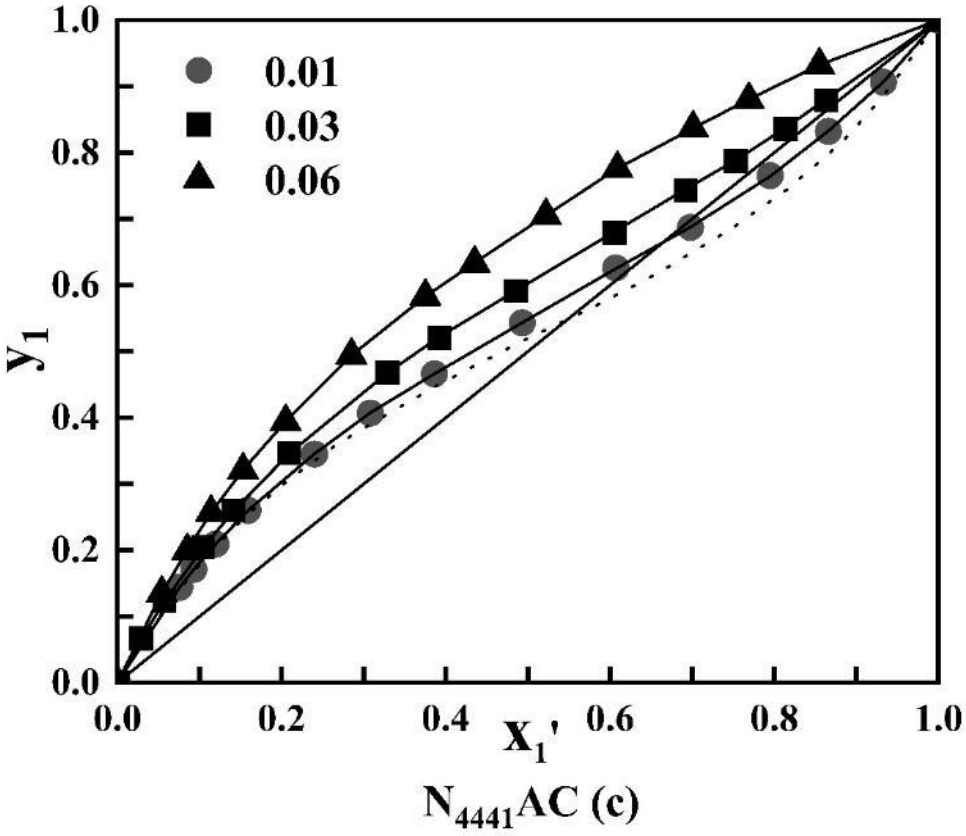

Fig. 3 x_1' - y_1 diagram for the ternary system of ethyl acetate (1) + ethanol (2) +IL{ [$N_{2,2,2,2}$][AC] (a), [EMMIM][AC] （b）, [$N_{4,4,4,1}$][AC] （c） }(3) at 101.3 kPa ; ▲, $x_3 = 0.06$; ■, $x_3 = 0.03$; ●, $x_3 = 0.01$; dashed line, $x_3 = 0$; solid line, NRTL model calculation value.

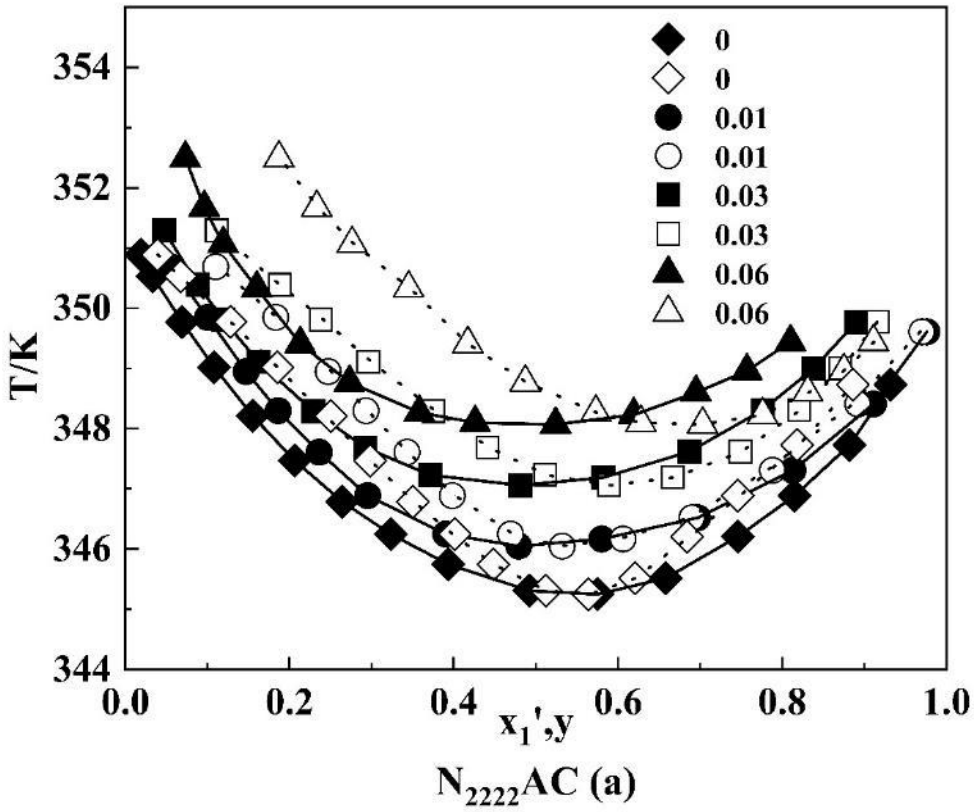
0
0
0.01
0.01
0.03
0.03
0.06
0.06
354
352
350
348
346
344
T/K
0.0
0.2
0.4
0.6
0.8
1.0
x1',y
N2222AC (a)

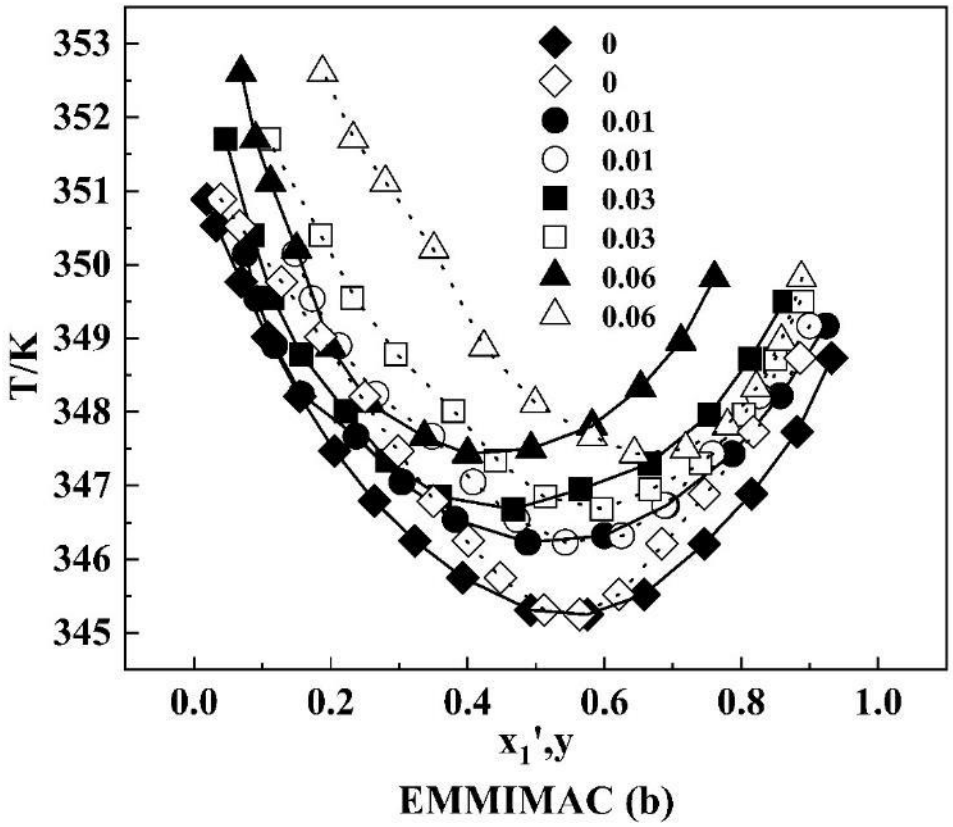
353
352
351
350
349
348
347
346
345
T/K
0.0
0.2
0.4
0.6
0.8
1.0
x1',y
0
0
0.01
0.01
0.03
0.03
0.06
0.06
EMMIMAC (b)

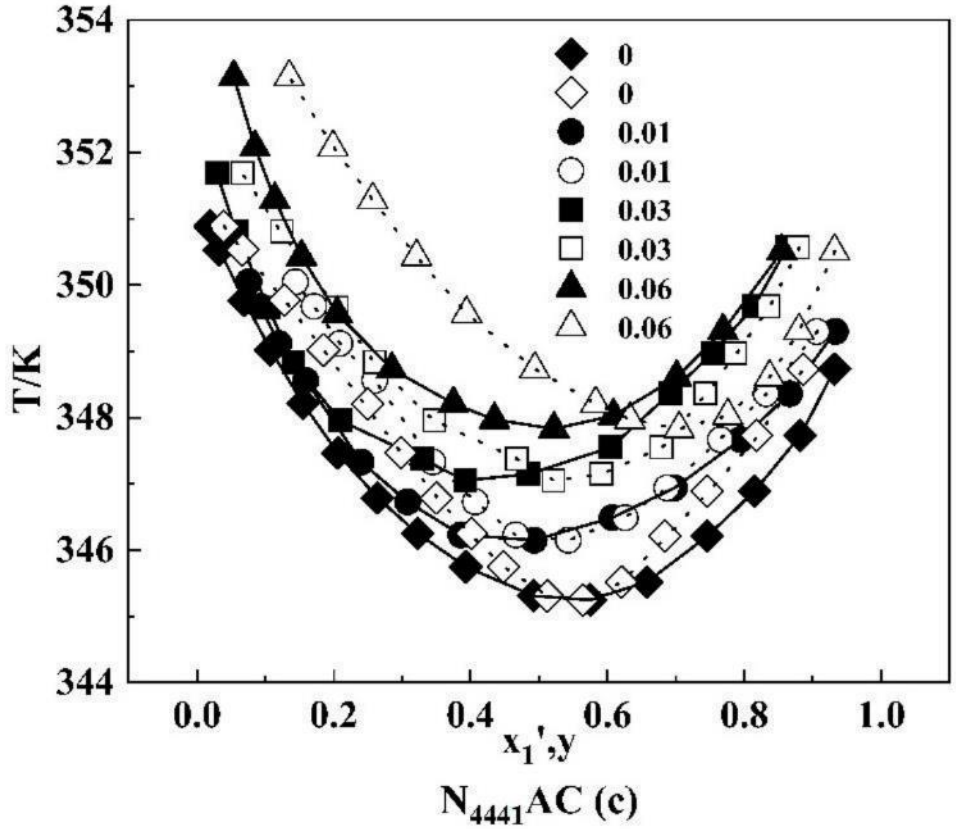

Fig. 4 T-x_1'-y_1 diagram for ternary system ethyl acetate (1) + ethanol (2) + IL{ [$N_{2,2,2,2}$][AC] （a）, [EMMIM][AC] （b）, [$N_{4,4,4,1}$][AC] (c) } (3) at 101.3 kPa: T-x_1' and T-y_1 (▲, Δ) x_3 = 0.06, (■, □) x_3 = 0.03, (●, ○) x_3 = 0.01; (◆, ◇) x_3 = 0; NRTL model calculation value (solid line) T-x_1', (dashed line) T-y_1.

In addition to minimum IL mole fraction to break azeotrope, average relative volatility ($\overline{\alpha_{12}}$) is also indispensable to judge the difference of volatility between light and heavy constituents caused by IL [36]. The higher the $\overline{\alpha_{12}}$ value, the greater the difference of volatility between light and heavy constituents, and the stronger the separation effect of IL. α_{12} is shown in Figure 5. After azeotrope is broken, $\overline{\alpha_{12}}$ listed in Table 8 is figured out through Eq. 6 and used to evaluate the difference of volatility between light and heavy constituents after azeotrope breaking. At the same IL content, the order of the $\overline{\alpha_{12}}$ value is $\overline{\alpha_{12}}$ [EMMIM][AC] > $\overline{\alpha_{12}}$ [$N_{2,2,2,2}$][AC] > $\overline{\alpha_{12}}$ [$N_{4,4,4,1}$][AC]. So the sequence of IL separation ability after azeotrope disappearing is [EMMIM][AC] > [$N_{2,2,2,2}$][AC] > [$N_{4,4,4,1}$][AC].The IL separation ability sequence is consistent with that of IL azeotrope breaking ability in this manuscript. Compared with [$N_{4,4,4,1}$] [AC] and [$N_{2,2,2,2}$][AC],[EMMIM][AC] has a better ability to separate the binary mixture. The experimental conclusion is consistent with the previous COSMOtherm software calculation result [38,39,47-49].

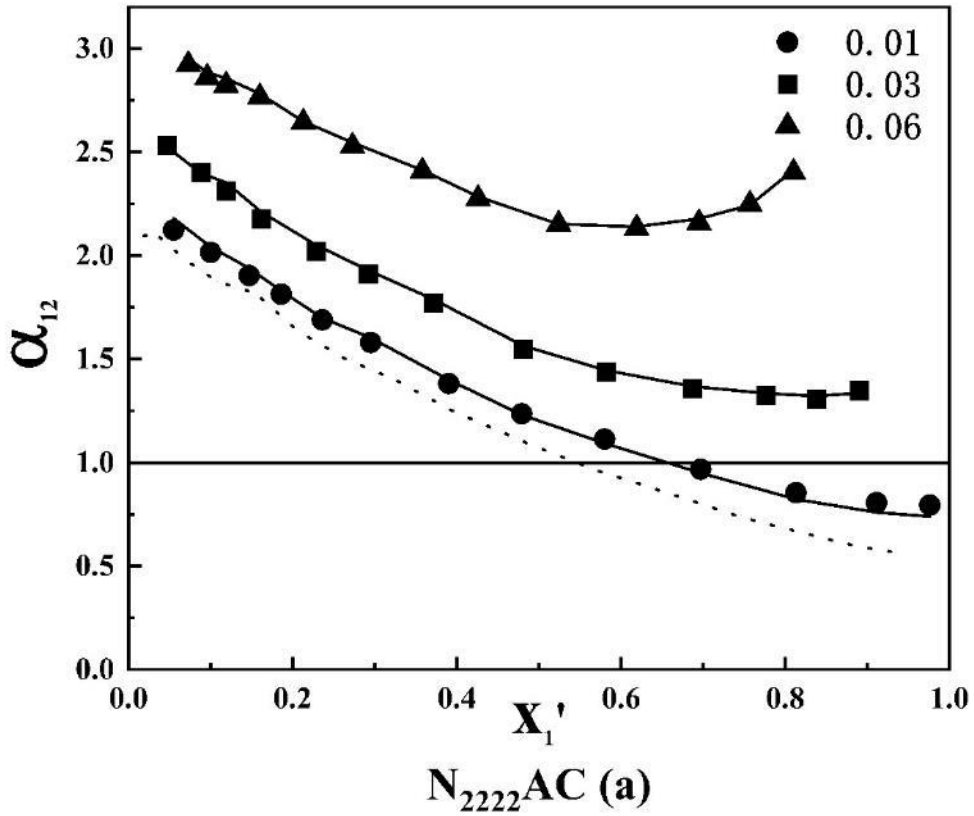
0. 01
0. 03
0. 06
3.0
2.5
2.0
1.5
1.0
0.5
0.0
0.0
0.2
0.4
0.6
0.8
1.0
α_{12}
X_1'
$N_{2222}AC$ (a)

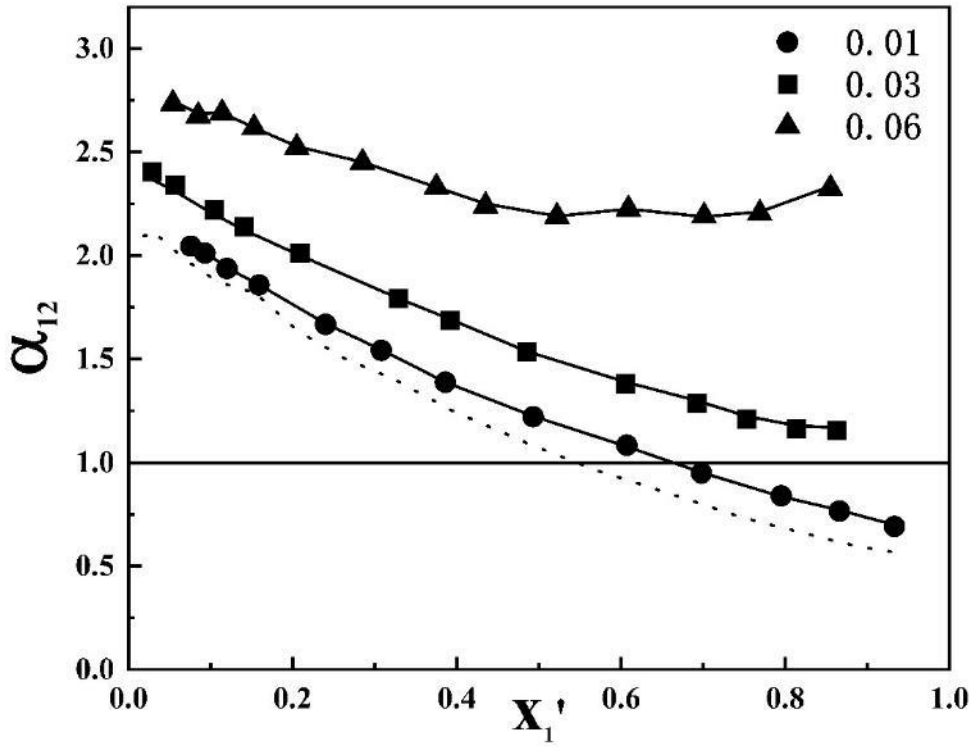

EMMIMAC (b)

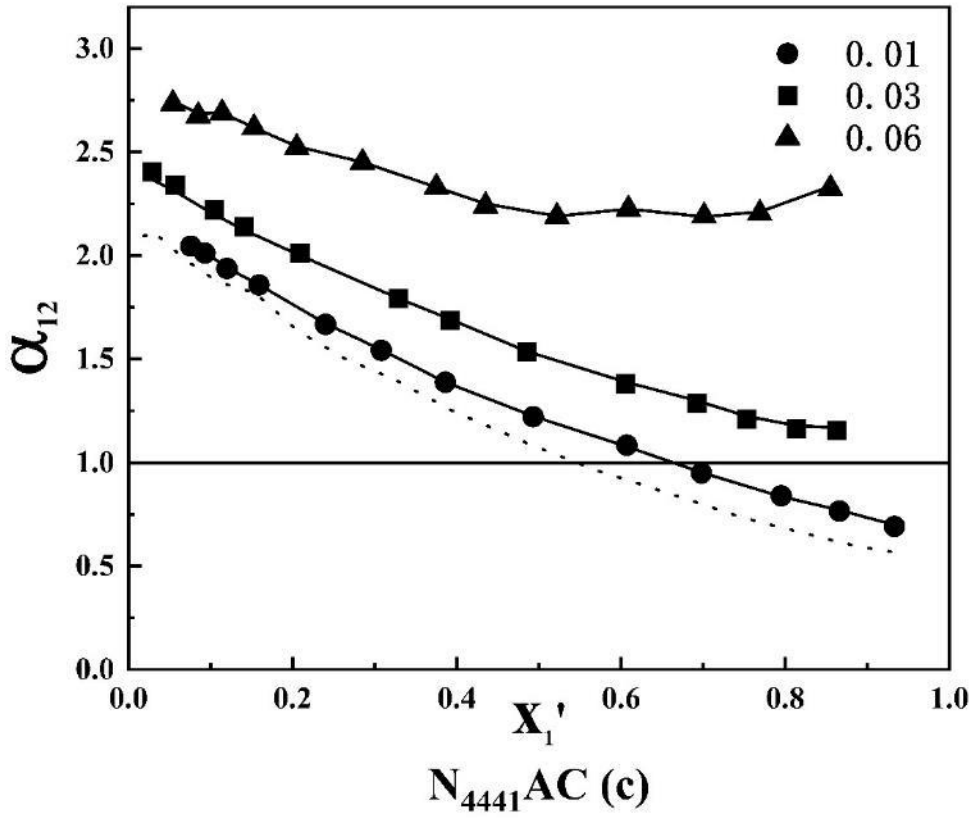

Fig. 5 Relative volatility of ethyl acetate (1) to ethanol (2) including {[$N_{2,2,2,2}$][AC] (a),[EMMIM][AC] (b),[$N_{4,4,4,1}$][AC] (c)} (3) at 101.3 kPa: ▲, $x_3 = 0.06$; ■, $x_3 = 0.03$;●, $x_3 = 0.01$;dashed line, $x_3 = 0$; solid line, NRTL model calculation value.

Table 8 The Average Relative Volatility

Constituent	Mole fraction	$\overline{\alpha_{12}}$
[$N_{2,2,2,2}$][AC]	0.06	2.485
	0.03	1.803
[EMMIM][AC]	0.06	2.785
	0.03	1.861
[$N_{4,4,4,1}$][AC]	0.06	2.414
	0.03	1.718

According to Eq.1, the volatility and the activity coefficients (γ) have the same trend of change. The greater the γ of the constituent, the higher the volatility [50]. γ1 and γ2 are calculated according to Eq.1 and illustrated in Figure 6-7. According to the figures, γ_1 changes in parallel with the change in IL content, while γ_2 has the opposite trend. It can be inferred that when IL content is increased, ethyl acetate volatility is increased, so it is more easily enriched in the vapor phase. Ethanol is just the opposite, thus allowing the two constituents to be more easily separated. Considering intermolecular hydrogen bonding interactions [13,14], it can be inferred that ethanol is more firmly bound by IL hydrogen bond into the liquid phase, while ethyl acetate is easier to enter the vapor phase because it is no longer bound by ethanol hydrogen bonding.

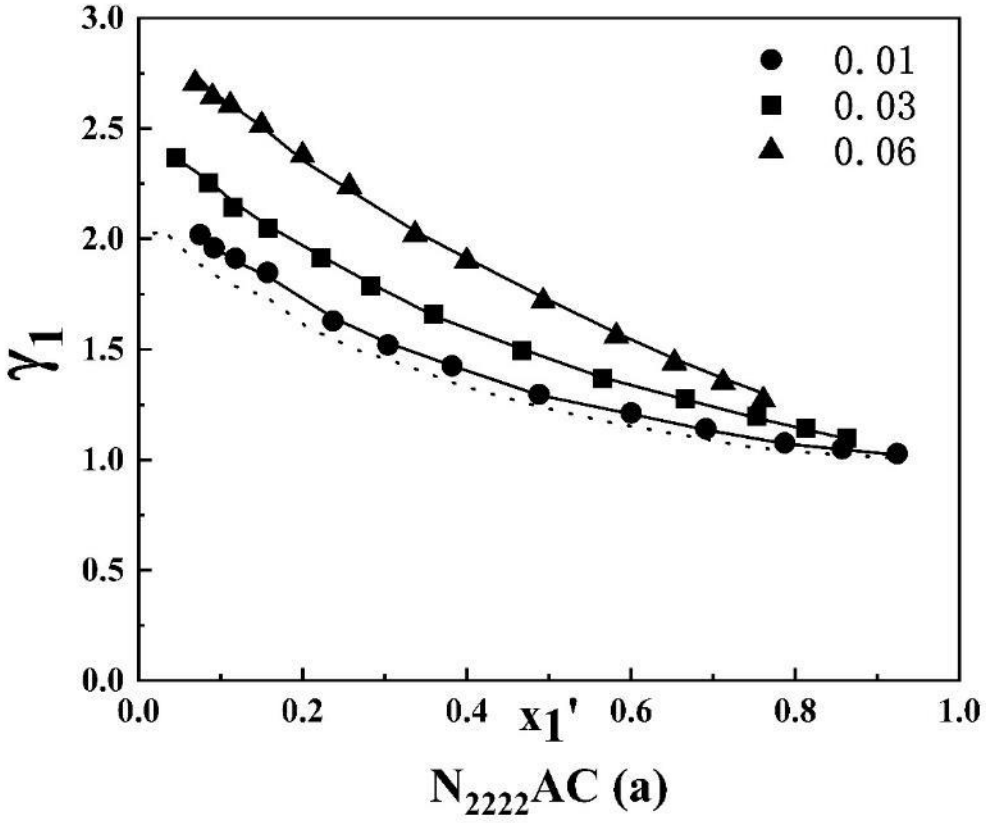
3.0
2.5
2.0
1.5
1.0
0.5
0.0
γ_1
0.0
0.2
0.4
0.6
0.8
1.0
x_1'
0.01
0.03
0.06
$N_{2222}AC$ (a)

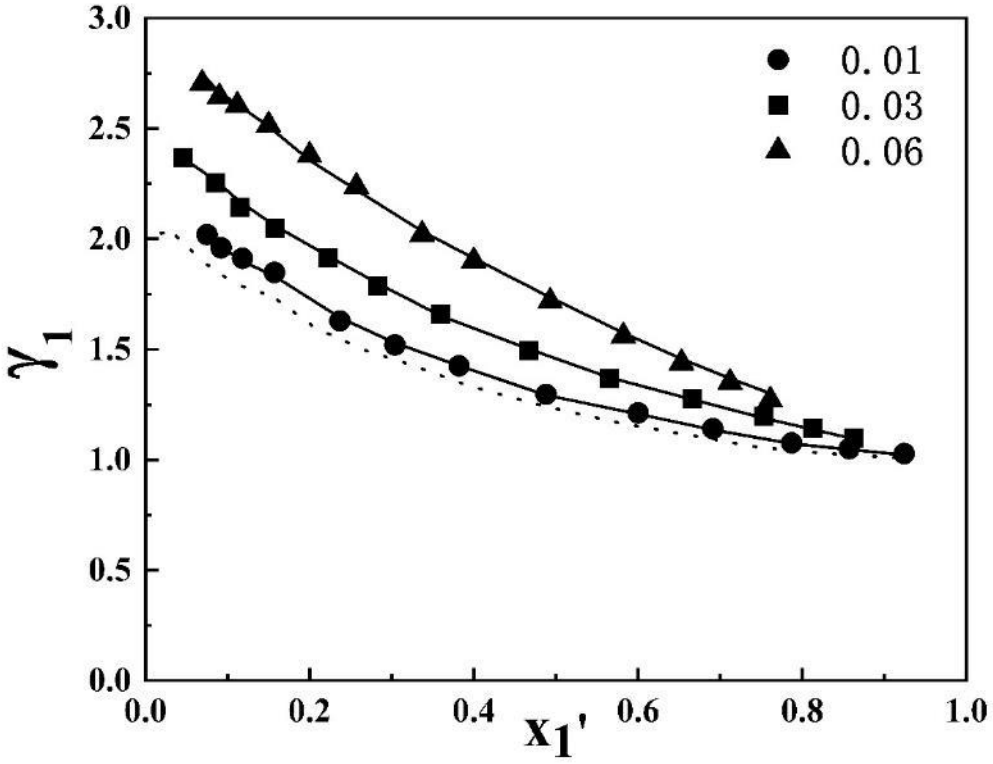

EMMIMAC (b)

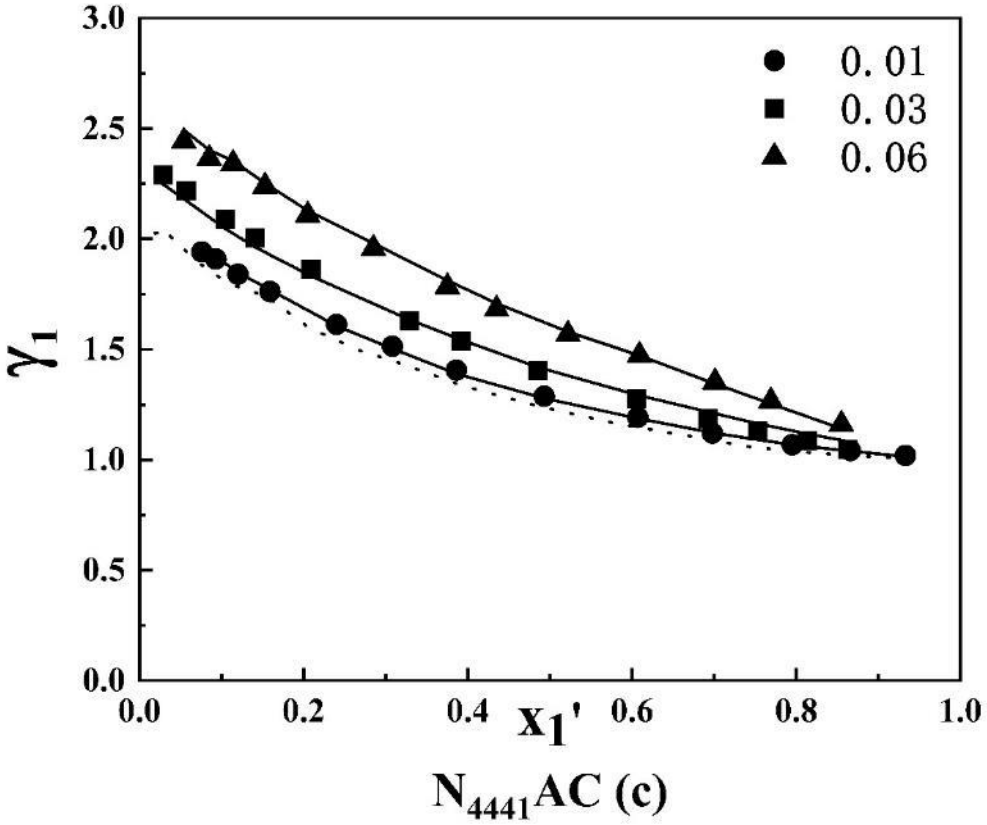

Fig. 6 Activity coefficients γ_1 of ethyl acetate (1) + ethanol (2) including { $[N_{2,2,2,2}][AC]$ (a),[EMMIM][AC](b),$[N_{4,4,4,1}][AC]$(c) } (3) at 101.3kPa: ▲, $x_3 = 0.06$; ■, $x_3 = 0.03$; ●, $x_3 = 0.01$; dashed line, $x_3 = 0$; solid line, NRTL model calculation value.

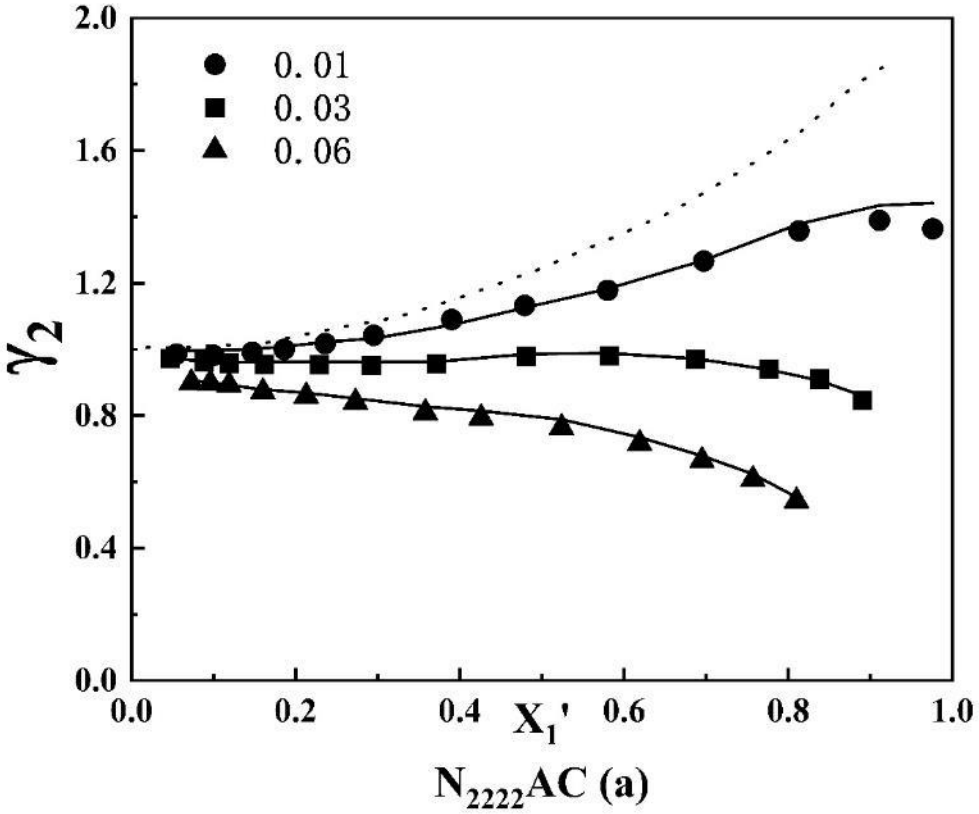
2.0
1.6
1.2
0.8
0.4
0.0
0.0
0.2
0.4
0.6
0.8
1.0
γ_2
X_1'
0.01
0.03
0.06
$N_{2222}AC$ (a)

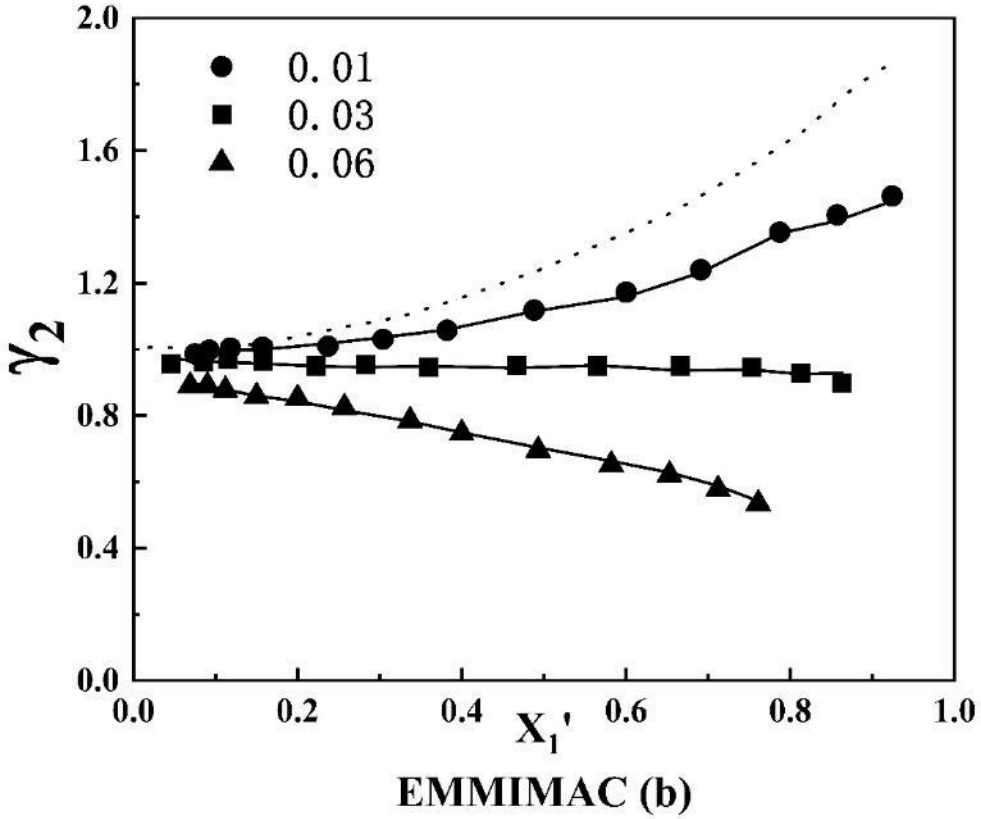

EMMIMAC (b)

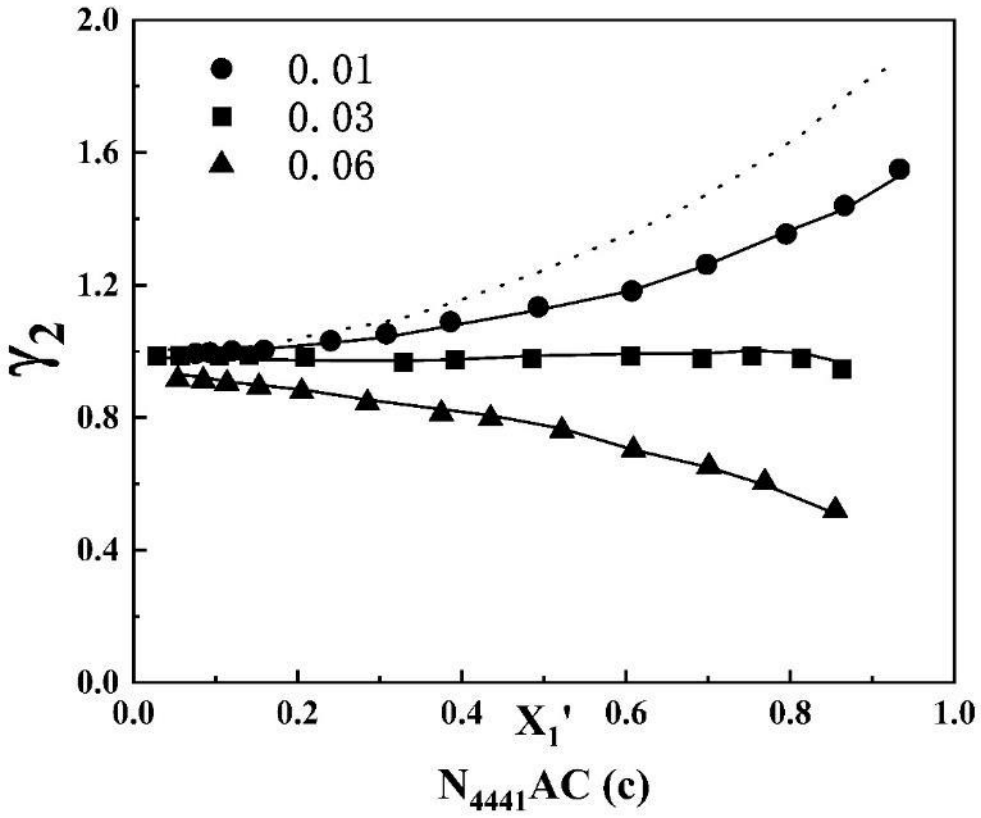

Fig. 7 Activity coefficients γ_2 of ethyl acetate (1) + ethanol (2) including { $[N_{2,2,2,2}][AC]$ (a),[EMMIM][AC] (b),$[N_{4,4,4,1}][AC]$ (c) } (3) at 101.3 kPa: ▲, $x_3 = 0.06$; ■, $x_3 = 0.03$; ●, $x_3 = 0.01$; dashed line, $x_3 = 0$; solid line, NRTL model calculation value.

3.3 σ-profile analysis

The σ-profiles of the molecules and ions involved in this work are illustrated in Figures 8 and 9, respectively. ILs separation abilities are related to the hydrogen bonds between them and the constituents to be separated. The strength of hydrogen bonds is mainly determined by the polar peak in the σ-profile. The greater polar peak area is, the greater hydrogen bonding force is. When the polar peak area is close to each other, the greater the non-polar peak area is, the smaller the hydrogen bonding force is.

Compared with the ethyl acetate peak, ethanol not only has peak in the donor region, but also has a smaller non-polar peak in Figure 8. According to Figure 9, $[Ac]^-$ shows acceptor peaks, while $[EMMIM]^+$, $[N_{2,2,2,2}]^+$ and $[N_{4,4,4,1}]^+$ show donor peaks. The non-polar peak area is $[EMMIM]^+ < [N_{2,2,2,2}]^+ < [N_{4,4,4,1}]^+$, while their donor peaks are similar. The polar peak area of ethanol or ethyl acetate is smaller than that of IL.

According to Figure 8 and Figure 9, any two constituents of IL, ethanol and ethyl acetate may be linked by hydrogen bond. The presence of hydrogen bond leads to azeotropy of the ethanol and ethyl acetate. Because ethanol has donor peaks and smaller non-polar peaks, it is better at forming hydrogen bonds than ethyl acetate. The smaller polar peak area of two molecules to be separated than that of the IL suggests that IL are more easily to form hydrogen bond than either of the two molecules, so the new hydrogen bond is formed between ethanol and IL after IL is added into ethanol and ethyl acetate solution. There is no azeotrope in the mixture because the

hydrogen bond that sustains their azeotrope is replaced by that between ethanol and IL [15,30].

The three ILs have the same anion, so their ability to break the azeotrope is only related to the structure of the cation. Because the polar peak areas of these cations are very similar, their separation ability is determined by non-polar peak area. the larger the non-polar peak area, the weaker the hydrogen bonding force and the weaker the separation ability. According to Figure 9, the separation ability order is [EMMIM][AC] > $[N_{2,2,2,2}]$[AC] > $[N_{4,4,4,1}]$[AC]. Consistent with the experimental conclusion.

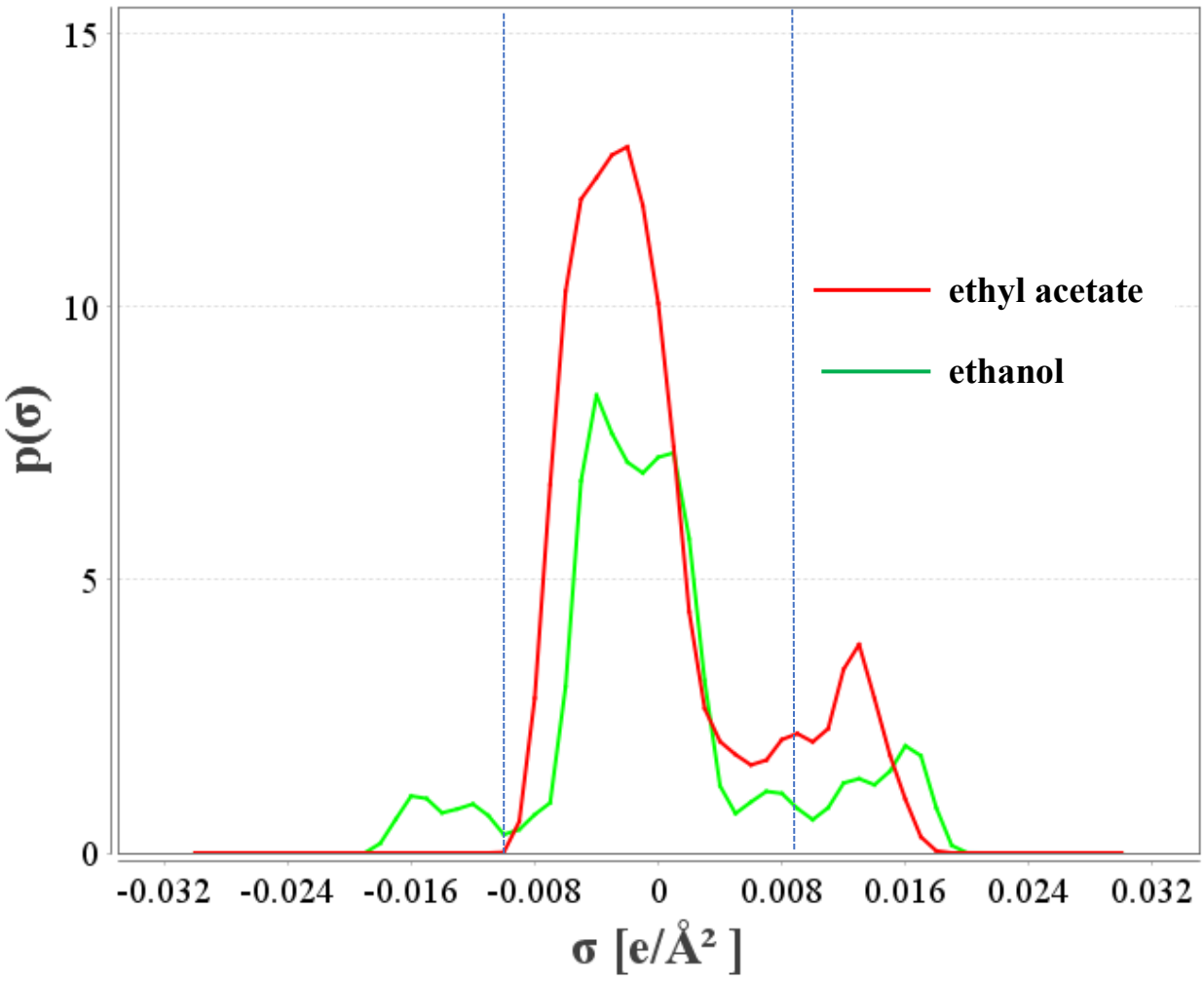

Fig. 8 σ-profiles for Ethyl acetate (1) + ethanol (2)

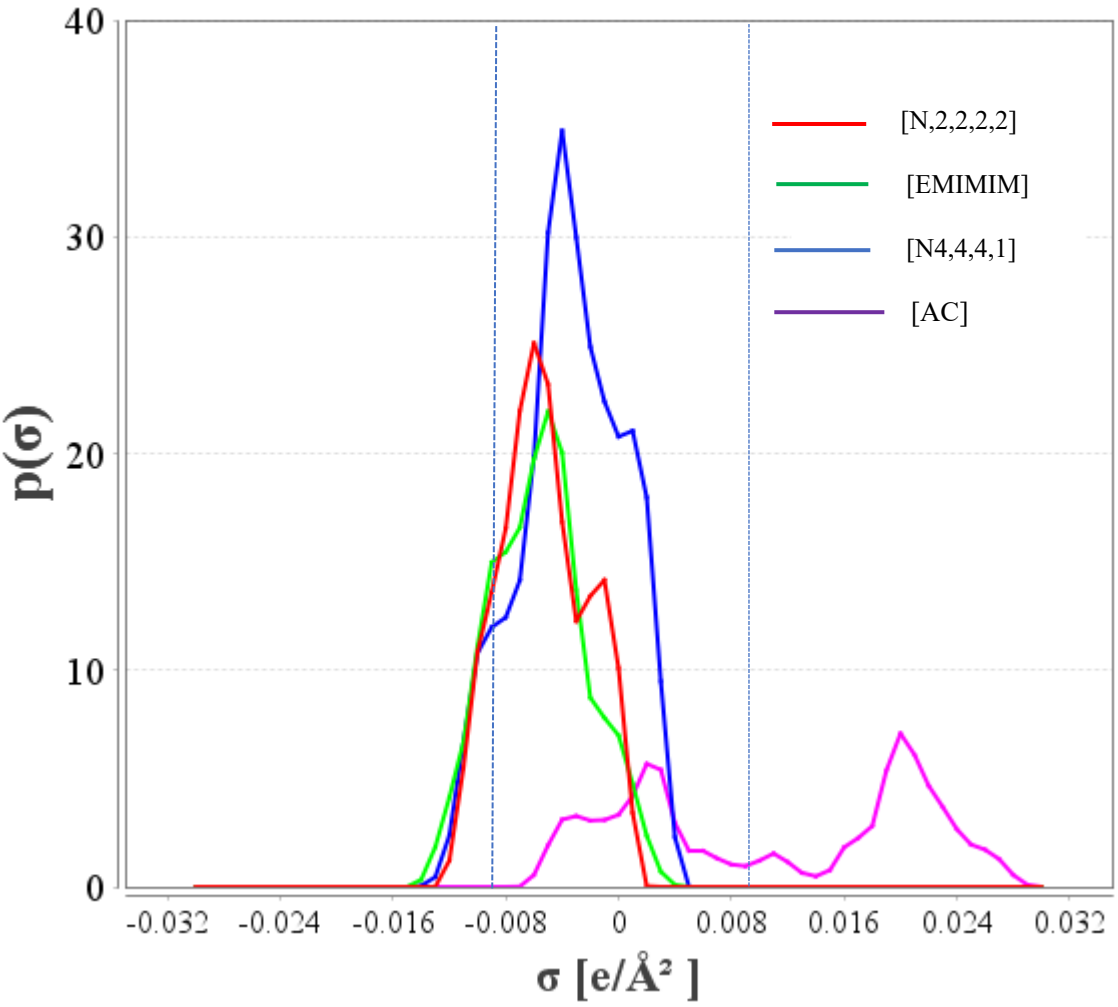

Fig. 9 σ-profiles for $[N_{4,4,4,1}]^+$, $[EMMIM]^+$, $[N_{2,2,2,2}]^+$, $[AC]^-$

4 CONCLUSION

The ethanol + ethyl acetate + IL ($[N_{2,2,2,2}][AC]$, [EMMIM][AC] or $[N_{4,4,4,1}][AC]$) ternary VLE data were gauged under normal pressure. The azeotropic point enhances with the enhance of IL concentration in the mixed solution. NRTL equation has a excellent correlation with experiment data. According to NRTL equation, for $[N_{2,2,2,2}][AC]$, [EMMIM][AC] and $[N_{4,4,4,1}][AC]$, minimum mole fractions for completely eliminating azeotrope are 0.015, 0.020 and 0.022, respectively. Compared to previously reported results, the better breaking azeotropic capacities are shown by the three ILs. Stronger hydrogen bonds have been formed between Ethanol and IL, which stronger bounds ethanol into the liquid phase. The strength order of the ethanol-IL hydrogen bonds formed by the three ILs is [EMMIM][AC] > $[N_{2,2,2,2}][AC]$ > $[N_{4,4,4,1}][AC]$. Outstanding separation effects have been shown by the three ILs. Among three ILs, [EMMIM][AC] shows the best separation ability.

Acknowledgments

This work is financially supported by the National Science Foundation of China (Project No. 22278272), the Scientific Research Project of the Education Department of Liaoning Province (Project No. LJKZ0426), the National Science Foundation of China (Project No. 21978173).

Declarations

The authors declare no competing financial interest.

REFERENCES

1. Wang, J.; Liu, W. B.; Tan, S. Y. Present Situation and Trend of Technology of Ethyl Acetate. Appl. Sci. Technol. **30**, 51–53 (2003**)**
2. Santacesaria, E.; Carotenuto, G.; Tesser, R.; Serio, M. D. Ethanol dehydrogenation to ethyl acetate by using copper and copper chromite catalysts. Chem. Eng. **179**, 209-220 (2012)
3. Tu, C.; Wu, Y.; Ou, F. Effect of 1,2-propanediol on the vapor-liquid equilibria of the ethyl acetate + ethanol system at 101.3 kPa. Fluid Phase Equilib. **130** (1), 243-252 (1997)
4. Li, Q.; Zhang, J.; Lei, Z.; Zhu, J.; Xing, F. Isobaric Vapor-Liquid Equilibrium for Ethyl Acetate + Ethanol + 1-Ethyl-3-methylimidazolium Tetrafluoroborate. J. Chem. Eng. Data **54**, 193–197 (2009)
5. Hu, X.; Li, Y.; Cui, D. Separation of ethyl acetate and ethanol by room temperature ionic liquids with the tetrafluoroborate anion. J. Chem. Eng. Data . **53**, 427-433 (2008)
6. Orchillés, A.V.; Miguel, P.J.; Vercher, E.; Andreu, A. Isobaric vapor-liquid equilibria for ethyl acetate+ ethanol + 1- ethyl-3- methylimidazolium trifluoromethanesulfonate. J. Chem. Eng. Data **52**, 2325-2330 (2007)
7. Li, W.; Zhang, L.; Guo, H.; Li, J.; Zhang, T. Effect of Ionic Liquids on the Binary Vapor−Liquid Equilibrium of Ethyl Acetate + Methanol System at 101.3 kPa. J. Chem. Eng. Data **64**, 34-41 (2019)
8. Li, W.; Yin, H.; Guo, H.; Li, J.; Zhang, T. Separation abilities of three acetate-based ionic liquids for benzene-methanol mixture through vapor-liquid equilibrium experiment at 101.3kPa. Fluid Phase Equilib. **492**, 80-87 (2019)
9. Zhang, Z.; Zhang, A.; Wu, K.; Zhang, Q.; Hu, A.; Li, W. Separation of ethyl acetate and 2-propanol azeotropic mixture using ionic liquids as entrainers. Fluid Phase Equilib. **429**, 331-338 (2016)
10. Li, W.; Xu, N.; Xu, H.; Zhang, A.; Zhang, Z.; Zhang, T. Isobaric vapor–liquid equilibrium for ternary mixtures of acetone + methanol + ionic liquids at 101.3 kPa. Fluid Phase Equilib. **442**, 20–27 (2017)
11. Orchillés, A. V.; Miguel, P. J.; Vercher, E.; Martínez-Andreu, A. Ionic Liquids as Entrainers in Extractive Distillation: Isobaric Vapor-Liquid Equilibria for Acetone + Methanol + 1-Ethyl-3-methylimidazolium Trifluoromethanesulfonate. J. Chem. Eng. Data **52**, 141-147 (2007)
12. Zhang, Z.; Lu, R.; Wang, C.; Zhang, Q.; Li, W. Separation of the Dimethyl Carbonate + Ethanol Mixture Using Imidazolium-Based Ionic Liquids as Entrainers. J. Chem. Eng. Data **2**, 1705-1714 (2020)
13. Li, W.; Yin, H.; Guo, H.; Li, J.; Zhang, T. Separation abilities of three acetate-based ionic liquids for benzene-methanol mixture through vapor-liquid equilibrium experiment at 101.3kPa. Fluid Phase Equilib. **492**, 80-87 (2019)
14. Zhu, W.; Li, Q.; Liu, B.; Cai, X.; Fan, Z. Effect of imidazolium-based ionic liquid on vapor–liquid equilibria of 2-propanol + acetonitrile binary system at 101.3 kPa. Fluid Phase Equilib. **409**, 383-387 (2016)
15. Perèiro, A. B.; Araújo, J.M.M.; Esperan, J.M.M.S.S.; Marrucho, I. M.; Rebelo, L.P.N. Ionic liquids in separations of azeotropic systems – A review. Chem. Thermodyn. **46**, 2-28 (2012)
16. Lei, Z.; Li, C.;Chen, B.; Extractive Distillation: A Review. Sep. Purif. Rev. **32**(2), 121-213(2003)

17. Zhu, R.; Taheri, M.; Lei, Z. Extension of the COSMO-UNIFAC Thermodynamic Model. Ind. Eng. Chem. Res. **59**, 1693−1701 (2020)
18. Dong, Y.; Huang, S.; Guo, Y.; Lei, Z. COSMO-UNIFAC model for ionic liquids. AIChE J. e16787 (2019)
19. Dong, Y.; Zhu, R.; Guo, Y.; Lei, Z. A United Chemical Thermodynamic Model: COSMO-UNIFAC. Ind. Eng. Chem. Res. **57**, 15954−15958 (2018)
20. Tan, X.; Chen, L; Li, X.; Xie, F. Effect of anti-solvents on the characteristics of regenerated cellulose from 1-ethyl-3-methylimidazolium acetate ionic liquid. Int.J. Biol. Macromol. **124**, 314-320 (2019)
21. Dhanalakshmi, J.; Sai, P.; Balakrishnan, A. R. Effect of Inorganic Salts on the Isobaric Vapor–Liquid Equilibrium of the Ethyl Acetate–Ethanol System. J. Chem. Eng. Data **58,** 3, 560–569 (2013)
22. Li, Q.; Zhang, J.; Lei, Z.; Zhu, J.; Zhu, J.; Huang, X. Selection of Ionic Liquids as Entrainers for the Separation of Ethyl Acetate and Ethanol. Ind. Eng. Chem. Res. **48**(19), 9006-9012 (2009)
23. Li, R.; Cui, X.; Zhang, Y.; Feng, T.; Cai, J. Vapor-liquid equilibrium and liquid-liquid equilibrium of ethyl acetate + ethanol + 1-ethyl-3-methylimidazolium acetate. J. Chem. Eng. Data **57**, 911-917 (2012)
24. Zhang, D.; Deng, Y.; Li, C.; Chen, J. Separation of Ethyl Acetate-Ethanol Azeotropic Mixture Using Hydrophilic Ionic Liquids. Ind. Eng. Chem. Res. **47**, 1995-2001 (2008)
25. Zhang, Z.; Wu, K.; Zhang, Q.; Zhang, T.; Zhang, D.; Yang, R.; Li, W. Separation of ethyl acetate and ethanol azeotrope mixture using dialkylphosphates-based ionic liquids as entrainers. Fluid Phase Equilib. **454**, 91-98 (2017)
26. Yue, K.; Zhou, W. Isobaric vapor–liquid equilibrium for ethyl acetate + ethanol with ionic liquids [MMIM][DMP] and [OMIM][PF6] as entrainers. J. Mol. Liquids. **348**, 118404 (2022)
27. W. Hunsmann, Verdampfungsgleichgewicht von Ameisensaure/Essigsaure-und von Tetrachlorkohlenstoff/Perchlorathylen-Gemi-schen. Vapourisation equilibria offormic acid/acetic acid and carbon tetrachloride/perchloroethylene mixtures. Chem. Irg.Tech. **39**, 1142-1145 (1967)
28. Chen, X.; Yang, B.; A. Abdeltawab, A.; S. Al-Deyab, S.; Yu, G.; Yong, X. Isobaric Vapor − Liquid Equilibrium for Acetone + Methanol +Phosphate Ionic Liquids. J. Chem. Eng. Data **60**, 612−620 (2015)
29. Zhang, Z.; Lu, R.; Zhang, Q.; Chen, J.; Li, W. COSMO-RS based ionic liquid screening for the separation of acetonitrile and ethanol azeotropic mixture. Chem. Technol. Biot. **95** (12), 91-98 (2020)
30. Andreatta, A. E.; Charnley, M. P.; Brennecke, J. F. Using Ionic Liquids To Break the Ethanol-Ethyl Acetate Azeotrope. ACS. Sustain. Chem. Eng. **10**, 3435-3444 (2015)
31. Dhanalakshmi, J.; Sai, P.; Balakrishnan, A. R. Study of Ionic Liquids as Entrainers for the Separation of Methyl Acetate–Methanol and Ethyl Acetate–Ethanol Systems Using the COSMO-RS Model. J. Ind. Eng. Chem. Res. **52** (46):16396-16405 (2013)
32. Xu, Y.; Li, T.; Peng, C.; Liu, H. Influence of C2-H of Imidazolium-Based Ionic Liquids on the Interaction and Vapor-Liquid Equilibrium of Ethyl Acetate + Ethanol System: [Bmim]BF4 vs [Bmmim]BF4. Ind. Eng. Chem. Res. **8**, 1-32 (2015)
33. Fadia, G.; Hassiba, B.;Shen, W. Separation of ethanol – water mixture by extractive distillation using pyridinium-based ionic liquid 1-ethyl-3-methylpyridinium ethylsulfate. Chem. Eng. Process. **173**, 108815 (2022)
34. Zhang, L.;Yuan,X.; Qiao, B.; Qi, R.; Ji, J. Isobaric Vapor−Liquid Equilibria for Water + Ethanol + Ethyl Acetate + 1-Butyl-3-methylimidazolium Acetate at Low Water Mole Fractions. J. Chem. Eng.

Data **53**, 7, 1595–1601 (2008)
35. Winnert, J. M.; Devi, V. K. P. J.; Brennecke, J. F. Using Dialkylimidazolium Ionic Liquids To Break the Methanol + Methyl Acetate Azeotrope. Ind. Eng. Chem. Res. **58**, 50, 22633–22639 (2019)
36. Li, W.; Fan, X.; Guo, H.; He, X.; Wang, L.; Zhang, T. Isobaric vapor-liquid equilibrium for 2-butanone + ethanol + acetate-based ionic liquids at 101.3 kPa. Fluid Phase Equilib. **552**,113298 (2022)
37. Li, H.; Sun, G.; Li, D.; Xi L.; Zhou, P.; Li, X.; Zhang, J.; Gao, X. Molecular interaction mechanism in the separation of a binary azeotropic system by extractive distillation with ionic liquid. Green Energy Environ. **6**, 329-338 (2021)
38. Tamal, B.; Manish, K. S.; Ashok, K. Prediction of Binary VLE for Imidazolium Based Ionic Liquid Systems Using COSMO-RS. Ind. Eng. Chem. Res. **45** (9), 3207-3219 (2006)
39. Li, J.; Yang, X.; Chen, K.; Zheng, Y.; Peng, C.; Liu, H. Sifting Ionic Liquids as Additives for Separation of Acetonitrile and Water Azeotropic Mixture Using the COSMO-RS Method. Ind. Eng. Chem. Res. **51** (27), 9376–9385 (2012)
40. Kang, J. W.; Diky, V.; Chirico, R. D.; Magee, J. W.; Muzny, C. D.; Abdulagatov, I.; Kazakov, A. F.; Frenkel, M. Quality assessment algorithm for vapor-liquid equilibrium data. J. Chem. Eng. Data **55**, 3631-3640 (2010)
41. Islam, M. R.; Chen, C. C. COSMO-SAC sigma profile generation with conceptual segment concept. Ind. Eng. Chem. Res. **54**, 4441–4454 (2015)
42. Renon, H.; Prausnitz, J. M. Local Composition Thermodynamic Excess Functions for Liquid Mixtures. Aiche. **14** (1), 135-144 (1968)
43. Taha, M. Designing new mass-separating agents based on piperazine-containing good's buffers for separation of propanols and water azeotropic mixtures using COSMO-RS method. Fluid Phase Equilib. **425**, 40-46 (2016)
44. Berg, L. Separation of ethyl acetate from ethanol by azeotropic distillation: US, US5993610 A[P]. (1999)
45. Levenberg, K. A method for the solution of certain non-linear problems in least squares. Quart. Appl. Math. **2**, 164-168 (1944)
46. Susial, P.; Sosa-Rosario, A.; Rios-Santana, R. Vapor Liquid Equilibria for Ethyl Acetate + Methanol at (0.1, 0.5 and 0.7) MPa Measurements with a New Ebulliometer. J. Chem. Eng. Data **55** (12), 5701–5706 (2010)
47. Klamt, A.; Jonas, V.; Bürger, T.; Lohrenz, J. C. W. Refinement and Parametrization of COSMO-RS. Phys. Chem. A. **102** (26), 5074–5085 (1998)
48. Gutiérrez, J. P.; Meindersma, G. W.; Haan, A. D. COSMO-RS-Based Ionic-Liquid Selection for Extractive Distillation Processes. Ind. Eng. Chem. Res. **51** (35), 11518–11529 (2012)
49. Shu, W.; Lin, S.; Watanasiri, S.; Chen, C. Use of GAMESS/COSMO program in support of COSMO-SAC model applications in phase equilibrium prediction calculations. Fluid Phase Equilib. **276**, 37-45 (2009)
50. Domańska, U.; Marciniak, A.; Kròlikowska, M.; Arasimowicz, M. Activity Coefficients at Infinite Dilution Measurements for Organic Solutes and Water in the Ionic Liquid 1-Butyl-3-methyl-pyridinium Trifluoromethanesulfonate. J. Chem. Eng. Data **55**, 3208–3211 (2010)
51. Gutiérrez, J. P.; Meindersma, G. W.; Haan, A. B. D. COSMO-RS-based ionic-liquid selection for extractive distillation processes. Ind. Eng. Chem. Res. **51**, 11518–11529 (2012)
52. Marciniak, A. Influence of cation and anion structure of the ionic liquid on extraction processes

based on activity coefficients at infinite dilution. A review, Fluid Phase Equilib. **294**, 213–233 (2010)

53. Qin, H. Wang, Z.; Zhou, T.; Song, Z. Comprehensive Evaluation of COSMO-RS for Predicting Ternary and Binary Ionic Liquid-Containing Vapor–Liquid Equilibria. Ind. Eng. Chem. Res. **60**, 48, 17761–17777 (2021)
54. Andrew, B.; Craig, C. Student Understanding of Liquid−Vapor Phase Equilibrium. J. Chem. Educ. **89** (6), 707–714 (2012)
55. Besler, B. H.; Merz, K.M.; Kollman, P.A. Atomic charges derived from semiempirical methods. J. Comput. Chem. **11** (4), 431–439 (1990)
56. Yaws, C.; Yang, H. To estimate vapor pressure easily, J. Hydrocarbon Processing. **68**, 65-70 (1989)
57. Stephenson, R.M.; Malanowski (Eds.), S. Handbook of the Thermodynamics of Organic Compounds. Springer Netherlands Dordrecht, (1987)
58. Li, W.; Guan, T.; Cao, Y.; Zhang, Y.; Zhang, T. Isobaric vapor-liquid equilibrium for toluene-methanol system including three ionic liquids with acetate anion at 101.3 kPa. Fluid Phase Equilib. **506** (15), 112412 (2020)
59. Aniya, V.; De, D.; Singh,; A. Satyavathi, B. Isobaric Phase Equilibrium of tert-Butyl Alcohol + Glycerol at Local and Subatmospheric Pressures, Volumetric Properties, and Molar Refractivity from 303.15 to 333.15 K of tert-Butyl Alcohol + Glycerol, tert-Butyl Alcohol + Water, and Water + Glycerol Bin. J. Chem. Eng. Data **61**, 1850–1863 (2016)
60. Li, W.; Xu, N.; Xu, H.; Zhang, A.; Zhang, Z.; Zhang, T. Isobaric vaporeliquid equilibrium for ternary mixtures of acetone + methanol + ionic liquids at 101.3 kPa. Fluid Phase Equilib. **442**, 20-27 (2017)
61. Wu, T.; Zhang, Q.; Xin, H.; Li, S.; Song, T.; Zhang, Z. Study on the selective separation of methanol and methyl ethyl ketone from the azeotropic system using ionic liquids and their separation mechanism. J. Mol. Liq. **34**, 117571 (2021)
62. Wu, T.; Yin, C.; Zhang, A.; Xin, H. Lv, M.; Lin, T.; Lu,Y. Wang, Y. Song, T.; Li, S.; Zhang, Q.; Zhang, Z. Study on the Isobaric Vapor–Liquid Equilibrium Behavior of the Methanol + Methyl Ethyl Ketone System Using Ionic Liquids as Extractants and Model Correlation. J. Chem. Eng. Data (2022)
63. Wisniak, J.; Ortega, J.; Fernández, L. A fresh look at the thermodynamic consistency of vapour-liquid equilibria data. J. Chem. Thermodynamics. **105**, 385-395 (2016)
64. Ma, Y.; Gao, J.; Li, M.; Zhu, Z.; Wang, Y. Isobaric vapour–liquid equilibrium measurements and extractive distillation process for the azeotrope of (N,N-dimethylisopropylamine + acetone). J. Chem. Thermodynamics. **122**, 154-161 (2018)
65. Liu, X.; Zhang, Y.; Li, M.; Li, X.; Li, G.; Wang, Y.; Gao, J. Isobaric Vapor−liquid Equilibrium for Three Binary Systems of Ethyl Acetate + Propyl Acetate, Ethyl Acetate + Propylene Carbonate,and Propyl Acetate + Propylene Carbonate at 101.3 kPa. J. Chem. Eng. Data **63** (5), 1588–1595 (2018)

Supplementary Files

This is a list of supplementary files associated with this preprint. Click to download.

- SupportingInformation.docx